HAL
open science

Tempering kinetics of the X10CrMoVNb9-1 martensitic steel

Farah Hanna, Guilhem Michel Roux, Olivier Asserin, Jean Christophe Brachet, René Billardon

To cite this version:

Farah Hanna, Guilhem Michel Roux, Olivier Asserin, Jean Christophe Brachet, René Billardon. Tempering kinetics of the X10CrMoVNb9-1 martensitic steel. Solid State Phenomena, 2011, 172-174, pp.845-850. 10.4028/www.scientific.net/SSP.172-174.845 . cea-02284975

HAL Id: cea-02284975

https://cea.hal.science/cea-02284975

Submitted on 14 Dec 2023

HAL is a multi-disciplinary open access archive for the deposit and dissemination of scientific research documents, whether they are published or not. The documents may come from teaching and research institutions in France or abroad, or from public or private research centers.

L'archive ouverte pluridisciplinaire **HAL**, est destinée au dépôt et à la diffusion de documents scientifiques de niveau recherche, publiés ou non, émanant des établissements d'enseignement et de recherche français ou étrangers, des laboratoires publics ou privés.

TEMPERING KINETICS OF THE X10CrMoVNb9-1MARTENSITIC STEEL

F. Hanna[1-4, a], G.-M. Roux[2, b], O. Asserin[1, c], J.-C. Brachet[3, d] & R. Billardon[4,e]

[1]CEA, DEN, DANS, DM2S, SEMT, LTA, F-91191 Gif sur Yvette, France.

[2]CEA, DRT, LITEN, DTH, LTH, F-38054 Grenoble Cedex 9, France.

[3]CEA-Saclay, DEN, Serv. Rech. Met. Appl., F-91191 Gif sur Yvette, France.

[4]LMT-Cachan, ENS Cachan/CNRS (UMR8535), F-94235 CACHAN, France.

[a]farah.hanna@cea.fr, [b]guilhem.roux@cea.fr, [c]olivier.asserin@cea.fr,
[d]jean-christophe.brachet@cea.fr, [e]Rene.Billardon@lmt.ens-cachan.fr

Key words: Martensitic steel; Carbides precipitation; Phase transformation kinetics; Thermo Electric Power, Martensite tempering, Non-isothermal heat treatments

Abstract

This work is part of a collaborative study between CEA-Saclay and LMT-Cachan on the numerical simulation of multi-pass GTA-Welding of thick specimens made of X10CrMoVNb9-1 (ASTM 387 or "T91") steel. The final objective of this paper is to exhibit the prediction capabilities of an improved version of the Thermo-Metallurgical-Mechanical "TMM" model for X10CrMoVNb9-1 martensitic steel (initially developed by G.-M. Roux). In this paper, focus is made on the modelling of the martensite tempering due to the complex thermal loadings induced by the multi-pass process. Herein, it has been chosen to study the tempering kinetics via the evolution of the free carbon content or, conversely, the carbides precipitation overall fraction, growth and dissolution. Thermo-Electric Power (TEP) measurements as well as hardening measurements have been used to investigate the tempering phenomenon. Measurements are fast to perform and are not very sensitive to the geometry of the material (in opposite to resistivity measurements). A phenomenological tempering model was developed and identified from several tests at constant tempering temperatures ranging from 550°C up to 750°C. The improved TMM model including this tempering model was used to perform the 2D finite element analysis of the 16-pass GTA welding process of a narrow groove butt-weld. The predictions are favourably compared with the "real" microstructure.

Introduction

The stability of this 9wt% chromium, 1wt% molybdenum martensitic steel – up to 750°C without mechanical loading – is sought for various high temperature applications.

The quantitative prediction of the microstructure state and residual stresses induced by a welding process requires the good knowledge of phase transformations kinetics [1]. Many works focus on carbides hardening contribution without mentioning the tempering impact on mechanical behaviour. The aim of this work is to study the tempering kinetic and its influence on thermo-mechanical behaviour [2].

Tempering of martensitic steels involves the segregation of carbon, the precipitation of carbides, the decomposition of retained austenite, and the recovery and recrystallization of the martensitic structure. All the processes occur simultaneously and evolve independently as function of the tempering temperature [3].

In the bibliographies, several techniques are used to determine the kinetic of tempering, among them the resistivity [4], the dilatometry [5,6], the calorimetry [6,7] , the Transmission Electron Microscopy (TEM) [8-10], the Energy Filtered Transmission Electron Microscopy (EFTEM) [11], the X-ray [7,8,10,12], Atom Probe Field Ion Microscopy (APFIM) [11,13], and the Electron Spectroscopic Imaging (ESI) [14]. Since carbides have only limited effect, hardly measurable at the global scale (e.g. with dimensional and thermal analysis), the ThermoElectric Power (TEP) [14-17] a less common technique has been investigated.

ThermoElectric Power and hardness measurements

To investigate the microstructure evolution occurring during the tempering of martensite, TEP measurements were performed after isothermal ageing treatments.

In order to have the same initial microstructure, X10CrMoVNb9-1 martensitic steel parallelepiped (2 × 2 × 12 mm3) samples were austenitized for 45min at 1020°C under controlled atmosphere of argon (Fig. 1a). The samples were then cooled in the oven to ambient temperature at a speed rate exceeding 600°C/s enough to obtain a 100% homogeneous quenched martensite. Samples were then tempered at different temperature ranging for 450°C to 750°C and for different tempering time [0s, 19800s] (See Fig. 1b).

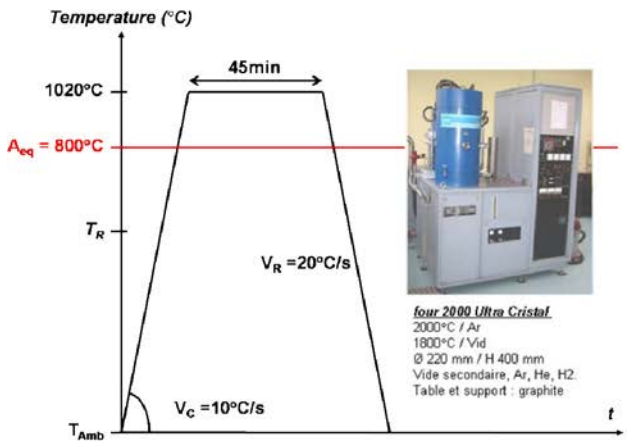

Fig. 1a: Austenization heat treatment

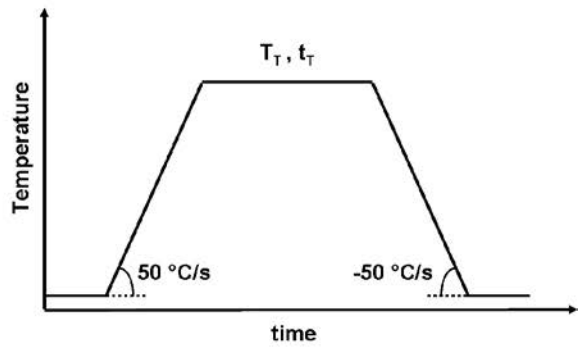

Fig. 1b: Tempering heat treatment

The principle of TEP measurements [17,19] is to establish a temperature gradient ΔT between the junctions of the studied alloy with two blocks of pure copper (see Fig. 2). A Potential voltage difference ΔV induced by the Seebeck effect can be then measured.

Blocks' temperatures are T and T + ΔT with T = 288 K and ΔT = 10 K. Where as the room temperature is 293 K. So the relative TEP (noted S) is defined as follows:

$$S = \Delta V / \Delta T$$

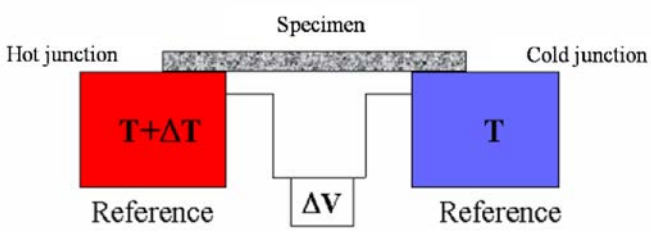

Fig. 2: TEP instrument illustration

Figure 3 represents the TEP measured values for the different time and temperature tempering. The TEP measurements uncertainty is estimated to 0.02 µV.K^{-1}.

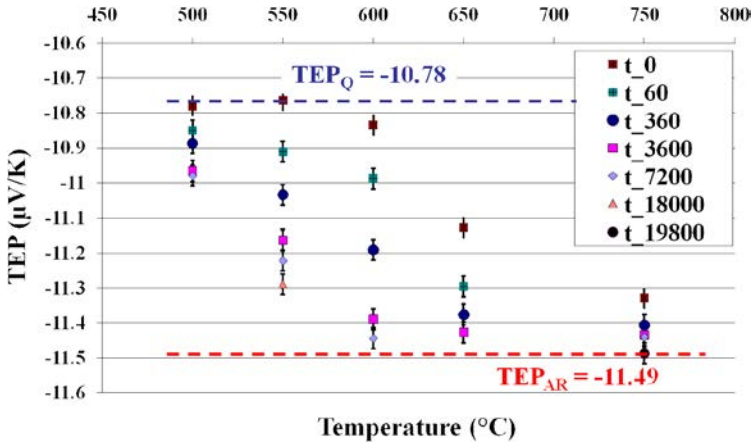

Fig. 3: TEP values for different tempering heat treatments

Tempering modelling

In order to achieve a model of tempering of martensite: the tempering of martensite is characterized by precipitation of carbon (presumably in the form of carbides MxCy) measured through the Thermo-Electric Power TEP [16]. Carbides influence the carbon content of martensite cause the precipitates take their carbon atoms from martensite. So the analysis of thermoelectric power evolutions, measured during isothermal tempering treatments, leads to a quantitative estimation of precipitate volume fraction.

An assumption was made that consist on relating the tempering state parameter 'x_T' to TEP measurements by the following linear expression:

$x_T = \dfrac{TEP - TEP_Q}{TEP_{AR} - TEP_Q}$ where '$TEP_{AR} = -11.4875$' is the TEP value for 'As Received' material (100% tempered) and '$TEP_Q = -10.78$' is the TEP value for the 'Quenched' martensite.

A Phenomenological model based on diffusion model was thought out.

$$\dot{x}_T = \frac{1}{n} D_0 \exp\left(-\frac{\Delta H}{R\,T}\right) x_T^{\,1-n} \left(1 - x_T\right) H\left[T - T_{TTh}\right] \qquad (1)$$

Where 'x_T' is the tempering state ($x_T = 0$ for quenched martensite and $x_T = 1$ for fully tempered martensite). 'D_0, n and ΔH' are material parameters and 'T_{TTh}' is the threshold tempering temperature under which no carbides precipitation can't take place.

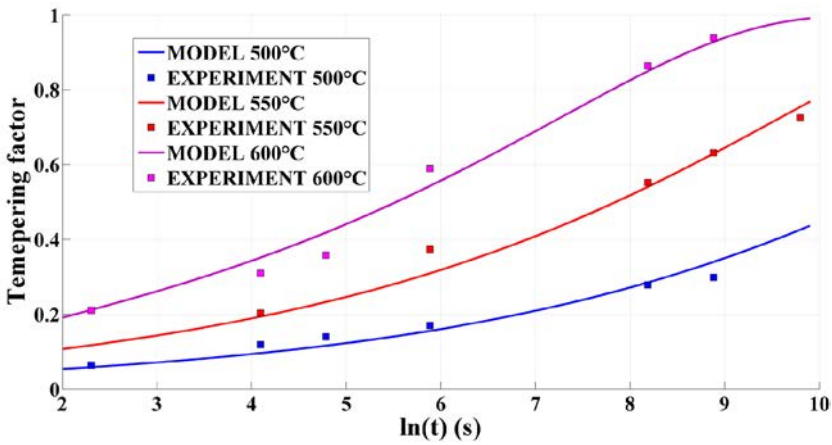

Fig. 3: Comparison between model and experiment after optimization.

The identified parameters are given in table 3.

Table 3: Identified tempering model parameters

D_0	ΔH	n	T_{TTh}
2.4 1013	278 KJ/mol	3.61	486°C

The ‘‘high”-temperature activation energy ΔH = 278 kJ mol-1 is close to that for activation diffusion energy for Chrome.

The analysis of TEP measurements at different times and temperatures (from 500 to 750 °C) shows that all processes occurring during tempering are related to (i) the self-diffusion activation energy of Chromium (activation energy of 3.51 eV = 339 kJ/mol [20]) driving the kinetics of carbide precipitation; and (ii) the mobility of dislocations and iron atoms (activation energy of 190 kJ mol^{-1}), driving the kinetics of recovery and coarsening of martensite lathes.

Hardness evolution

The same parallelepiped samples were subject to hardness measurements. The samples were wrapped with a hard resin to facilitate the measurements. Measurements were done using the hardness tester machine 'Struers, Duramin-A300'. A test load of 1 kgf was used. For each sample a series of ten measurements were performed to verify the homogeneity of the material. The starting point and test series were easily selected using the macro option of the observation camera. The fully automatic evaluation of hardness ensures the repeatability and limits human' mistakes. The uncertainty or error is estimated to 2%.

Results show a direct influence of tempering and carbides precipitations on hardness [6,11,21]. During tempering, the hardness drop due to carbides precipitation. Carbides have a little hardening effect compared to the one of the carbon trapped in the martensite matrix. The following phenomenological model relating to hardness to the tempering state 'x_T' was identified:

$HV_{TM} = HV_{AR} + \left(HV_Q - HV_{AR}\right)\exp\left(\frac{x_T - 1}{x_0}\right)$ where 'HV_{TM}' is the Tempered Martensite Vickers Hardness, 'HV_{AR}' is the As Received material (fully tempered) Vickers Hardness, 'HV_Q' is the Quenched martensite Vickers Hardness, and 'x_0' is a material parameter.

Table 4: Identified Hardness model parameters

HV_{AR}	HV_Q	x_0
185 HV	513 HV	0.374

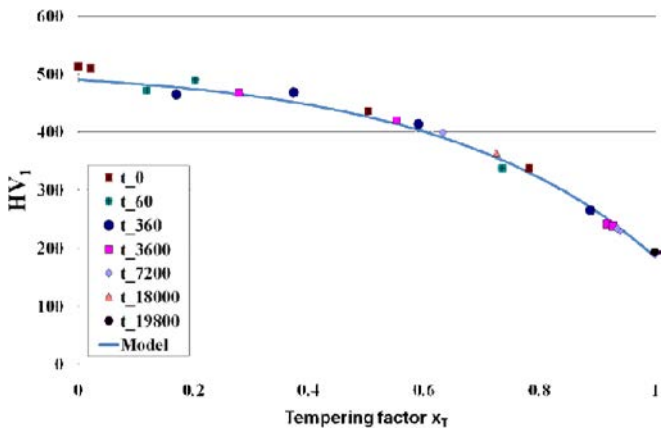

Fig. 4: Hardness vs tempering fraction evolution

Figure 4 shows experiment and modelled hardness vs tempering state evolutions.

Model validation

A real narrow groove gas tungsten arc multi-pass welding experiment was simulated using the finite element CEA code 'Cast3M' [22,23]. The above models were implemented under Matlab© and the thermal results of the previous simulation were used as inputs. The hardness profiles across (Fig 6) and through the different welding passes (fig. 7) were computed and compared to real measurements.

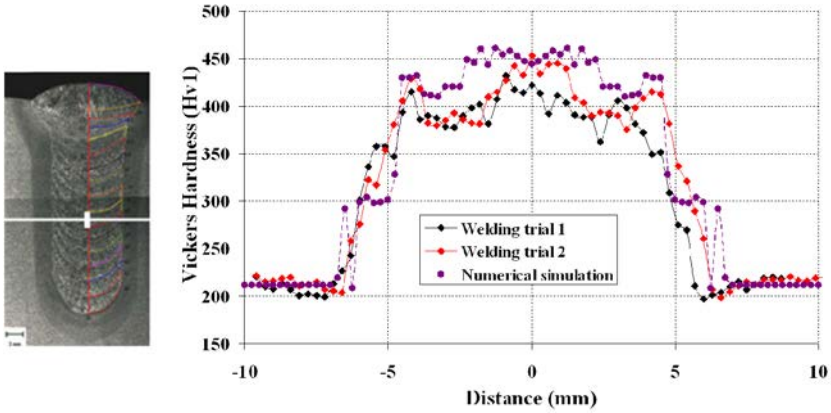

Fig. 6: Simulated and measured hardness profile across the seventh welding pass

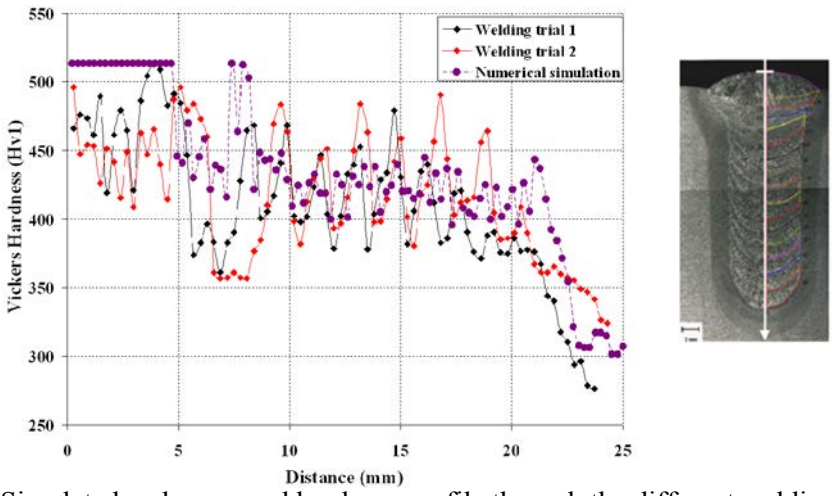

Fig. 7: Simulated and measured hardness profile through the different welding passes

After successive passes, the resultant microstructure is very heterogeneous, different more or less tempered martensite phases can co-exit. In order to solve this problem and only have one equivalent tempered martensite phase that coexists alone with the quenched martensite phase, a simple homogenisation law is performed:

$x_{T_{eq}} = \sum_{1=1}^{n} x_{T_i} y_{Q_i}$ and $y_{Q_T} = \sum_{1=1}^{n} y_{Q_{T_i}}$ where '$x_{T_{eq}}$' denotes the equivalent tempering state of the total tempered martensite phases 'y_{Q_T}' and '$y_{Q_{T_i}}$' denotes a martensite phase that has been more or less 'x_{T_i}' tempered.

This assumption seems logical since tempering is a cumulative problem. The hardness of the resultant mixture of quenched and tempered martensite is then assessed as followed:

$HV = y_Q\, HV_Q + \left(1 - y_Q\right)\left[HV_{AR} + \left(HV_Q - HV_{AR}\right)\exp\left(-\frac{x_{T_{eq}}}{x_0}\right)\right]$ where 'y_Q' denotes the quenched martensite fraction.

Small scatters can be observed between the hardness measured profiles of the two different trials. One can note that the general trend is found and the computation results are very close to reality.

Discussion

TEP has been successfully used, to characterize the microstructural evolution occurring during the tempering of martensite. In this, paper, TEP has been showed to be a alternative method to study martensite steel tempering.

References

[1] A. Schneider, G. Inden: Acta Mater, Vol. 53, No 2, (2005), p. 519

[2] A. Kostka, K.-G. Tak, R.J. Hellmig, Y. Estrin, G. Eggeler: Acta Mater, Vol. 55, (2007), p. 539

[3] E. Valencia Morales, N.J. Galeano Alvarez, J. Vega Leiva, L.M. Castellanos, C.E. Villar, R.J. Hernandez: Acta Mater, Vol. 52, (200), p. 1083

[4] G.-R. Speich: Transactions of the metallurgical society of AIME, Vol. 245, (1969), p. 2553

[5] C. Aubry: PhD thesis, L'Institut National Polytechnique de Lorraine, France, 1998.

[6] L. Cheng, E.-J. Mittemeijer: MMTA, Vol. 21, No. 1, (1990), p.13

[7] L. Cheng, A. Böttger, E.-J. Mittemeijer: MMTA, Vol.23, No. 4, (1992), p.1129

[8] J. Pesicka, R. Kuzel, A. Dronhofer, G. Eggeler: Acta Mater, Vol. 51, (2003), p. 4847

[9] P.-J. Ennis, A. Zielinska-Lipiec, O. Wachter, A. Czyrska-Filemonowicz: Acta Mater, Vol. 45, No. 12, (1997), p. 4901

[10] R. Agamennone, W. Blum, C. Gupta, J.-K. Chakravartty: Acta Mater, Vol. 54, (2006), p. 3003

[11] R.-C. Thomson, M.-K. Miller: Acta Mater, Vol. 46, (1998), p. 2203

[12] P.-R. Jemian, J.-R.Weertman, G.-G. Long, R.-D. Spal: Acta Metall Mater, Vol. 39, No. 11, (1991), p. 2477

[13] M. Hättestrand, H.-O. Andren: Acta Mater, Vol. 49, (2001) p. 2123

[14] F. Hofer, P. Warbichler, W. Grogger: Ultramicroscopy, Vol. 59, (1995), p. 15

[15] M. Perez, C. Sidoroff, A. Vincent, C. Esnouf: Acta Mater, Vol. 57, (2009), p. 3170

[16] J.-C Brachet: Workshop-Thermoelectricity,-INSA-Lyon, (2002)

[17] M. Houze: PhD thesis, L'Institut National des Sciences Appliquées de Lyon, (2002)

[18] J.-C. Brachet: Journ. de Phys. IV, Colloque C8, suppl. au Journ. de Phys. III, Vol. 5, (1995)

[19] F.-J. Blatt, P.-A. Schroeder, C.-L. Foiles CL, D. Greig: Plenum Press, (1976)

[20] J.-L. Campbell, C.-W. Schulte: Appl. Phys, Vol. 19, (1976), p.149

[21] F. Ernst, Y. Cao, G.-M. Michal: Acta Mater, Vol. 52, (2004) p.1469

[22] G.-M. Roux: PhD thesis, Paris 6 university, LMT-Cachan, (2007)

[23] http://www-cast3m.cea.fr